


RESEARCH ARTICLE

Open Access



Genome-wide exploration and characterization of miR172/euAP2 genes in *Brassica napus* L. for likely role in flower organ development

Tengyue Wang, Xiaoke Ping, Yanru Cao, Hongju Jian, Yumin Gao, Jia Wang, Yingchao Tan, Xinfu Xu, Kun Lu, Jiana Li and Liezhao Liu* 

Abstract

Background: *APETALA2*-like genes encode plant-specific transcription factors, some of which possess one microRNA172 (miR172) binding site. The miR172 and its target *euAP2* genes are involved in the process of phase transformation and flower organ development in many plants. However, the roles of miR172 and its target *AP2* genes remain largely unknown in *Brassica napus* (*B. napus*).

Results: In this study, 19 *euAP2* and four miR172 genes were identified in the *B. napus* genome. A sequence analysis suggested that 17 *euAP2* genes were targeted by Bna-miR172 in the 3' coding region. *EuAP2*s were classified into five major groups in *B.napus*. This classification was consistent with the exon-intron structure and motif organization. An analysis of the nonsynonymous and synonymous substitution rates revealed that the *euAP2* genes had gone through purifying selection. Whole genome duplication (WGD) or segmental duplication events played a major role in the expansion of the *euAP2* gene family. A cis-regulatory element (CRE) analysis suggested that the *euAP2*s were involved in the response to light, hormones, stress, and developmental processes including circadian control, endosperm and meristem expression. Expression analysis of the miR172-targeted *euAP2*s in nine different tissues showed diverse spatiotemporal expression patterns. Most *euAP2* genes were highly expressed in the floral organs, suggesting their specific functions in flower development. *BnaAP2-1*, *BnaAP2-5* and *BnaTOE1-2* had higher expression levels in late-flowering material than early-flowering material based on RNA-seq and qRT-PCR, indicating that they may act as floral suppressors.

Conclusions: Overall, analyses of the evolution, structure, tissue specificity and expression of the *euAP2* genes were performed in *B.napus*. Based on the RNA-seq and experimental data, *euAP2* may be involved in flower development. Three *euAP2* genes (*BnaAP2-1*, *BnaAP2-5* and *BnaTOE1-2*) might be regarded as floral suppressors. The results of this study provide insights for further functional characterization of the miR172 /*euAP2* module in *B.napus*.

Keywords: *Brassica napus*, miR172, *euAP2*, Evolution, Expression analysis

* Correspondence: liezhao@swu.edu.cn

College of Agronomy and Biotechnology, Chongqing Engineering Research Center for Rapeseed, Academy of Agricultural Sciences, State Cultivation Base of Crop Stress Biology for Southern Mountainous Land, Southwest University, Chongqing, China



Background

MicroRNAs are a class of endogenous, small non-coding RNAs (20–24 nucleotides) with critical roles in the post-transcriptional regulation of gene expression [1]. Plant miRNAs have been reported to be involved in many biological processes, such as auxin signalling [2], flowering time regulation [3], leaf development [4] and stress responses [5, 6]. Recent studies have also indicated that miRNAs can regulate developmental timing and floral induction in a variety of plants via their corresponding target genes [7–13]. In particular, two highly conserved microRNAs, namely, miR156 and miR172, have been identified as master regulators of vegetative phase change [14–19].

MiR172 was first obtained by small-RNA sequencing in *Arabidopsis* and has been found in many plants because of its high conservation [20]. The miR172 family is a major component of the age pathway, and it is encoded by MIR172a-e genes in *Arabidopsis*. The target genes of this family in *Arabidopsis* include six *APETALA-2* (*AP2*)-type genes: *APETALA2* (*AP2*), *TARGET OF EAT 1* (*TOE1*, *TOE2*, and *TOE3*), *SCHLAFMUTZE* (*SMZ*) and *SCHNARCHZAPFEN* (*SNZ*). *AP2* is involved in floral organ formation, and the other five *AP2*-like genes are mainly floral suppressors [3, 21, 22]. The *AP2* proteins have one or more *AP2* domains consisting of 60–70 highly conserved amino acids (aa) and two conserved components, namely, the YRG and RAYD motifs, at the N- and C-terminus of the *AP2* domain respectively [23–25].

MiR172 and its target genes play key roles in flowering time and floral organ differentiation. In *Arabidopsis*, overexpressing all the miR172 target genes except *TOE3* led to delayed flowering [18, 22, 24]. In contrast, the *toe1toe2* double mutant, *toe1toe2smzsnz* quadruple mutant and *toe1toe2toe3smzsnzap2* sextuple mutant all showed early flowering, and the flowering time advanced as the number of mutant genes increased [26, 27]. On the one hand, this result showed functional redundancy among the *AP2* genes; on the other hand, it confirmed that *AP2* genes negatively regulate flowering time in *Arabidopsis*. In the maize mutant *glossy15* (*gl15*), young leaves showed premature adult leaf characteristics because miR172-targeted *GL15* played a role in the juvenile to adult transition [28]. Overexpressing miR172 not only accelerated flowering but also resulted in abnormal flower development in *Arabidopsis* including a loss of petals and homologous transformation of sepals to carpels [3, 22, 26], the phenotype similar to the *ap2* mutant. When a 6-base mutation was introduced at the miR172 binding site of *AP2* to produce a miR172 resistance gene, a large number of petals were generated and the stamens were degenerated [22]. Overexpression of miR172b in rice delayed the transition from spikelet

meristem to floral meristem and resulted in homeotic transformation in floral organs [29]. Overexpression of miR172 in tobacco also resulted in the conversion of sepals to petals, while *35S::AP2m3* plants exhibited floral patterning defects that included the proliferation of numerous petals, stamens and carpels [30]. In barley, *Cleistogamy1* (*Cly1*) replaces the synonymous nucleotides at the miR172 target site and leads to the failure of flowering and a closed-fertilization phenotype [31].

Brassica napus is the second largest oil crop in the world. This species is an allopolyploid (AACC, $2n = 4x = 38$) that evolved from a natural interspecies cross between *Brassica rapa* (genome AA, $2n = 20$) and *Brassica oleracea* (genome CC, $2n = 18$) [32]. Flowering represents the transition from the vegetative stage to the reproductive stage. Flowering appropriately is crucial to ensure reproductive success and thus determines the growth period, yield and seed quality in *B. napus*. Despite the roles of *AP2* genes in *Arabidopsis* has been well described, the roles of miR172 and its target *AP2* genes in determining flowering and floral development are still unclear in *B. napus*. Although the MiRNA172c-*APETALA2-1* node has been identified as a key regulator of nitrogen fixation in common bean [33], the interaction between the *AP2* and MiR172 in *B. napus* has not clearly understood. Therefore, it would be intriguing to perform a genome-wide functional analysis of miR172/*euAP2* in *B. napus*. In this study, we systematically analysed the chromosomal location, evolutionary relationships, duplication events, collinearity, gene structure, conserved motifs and upstream cis-elements among miR172 members and their *euAP2* target genes. RNA sequencing (RNA-seq) and quantitative real-time PCR (qRT-PCR) were also carried out to analyse the expression pattern of *euAP2s* in diverse tissues and developmental stages.

Results

Identification of *euAP2* and miR172 genes in *B. napus*

Eight characterized *AP2* protein sequences in *Arabidopsis* were used as the query sequences to identify the *euAP2* gene family in the *B. napus* genome using BLASTP searches with an E-value of $\leq 10^{-10}$, and 19 putative *euAP2* family genes were identified. Then, the SMART, Pfam, CDD and HMMER databases were used to verify the *AP2* domains, and all 19 predicted protein had one or two *AP2* domains. As shown in Table 1, we numbered the *B. napus euAP2* according to their closest *Arabidopsis* homolog.

The chromosome location, protein sequence length, molecular weight (MW), isoelectric point (pI), and subcellular localization were analysed. The size of the *euAP2* proteins ranged from 103 (BnaTOE1–5) to 454 (BnaTOE2–3) amino acids. The predicted Mw of these deduced proteins varied from 11.00 kDa to

Table 1 List of putative *euAP2* genes and their protein features in *B.napus*

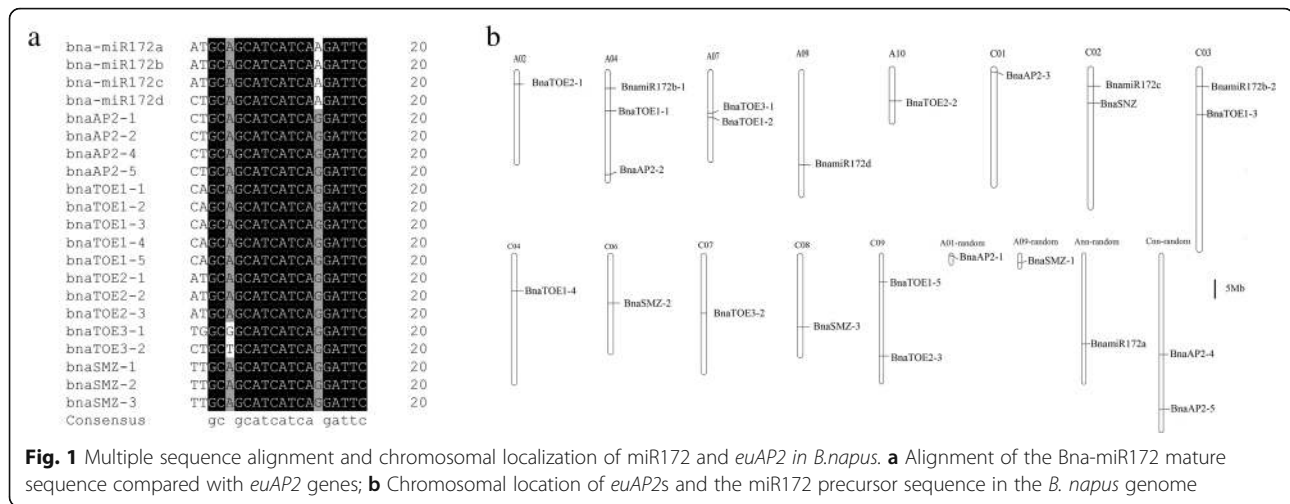
Gene id	Gene name	Gene id	Gene name	Chromosome	Target_start	Target_end	Amino acid length (aa)	pI	MW	Subcellular location	Conserved AP2 motif number
AT4G36920	<i>AthAP2</i>	BnaA01g34730D	<i>BnaAP2-1</i>	A01_random	581	601	233	8.89	25769.56	Nucleus	1
		BnaA03g53830D	<i>BnaAP2-2</i>	A03	1344	1364	432	6.77	47937.77	Nucleus	2
		BnaC01g01710D	<i>BnaAP2-3</i>	C01	–	–	400	6.02	44092.70	Nucleus	2
		BnaCnng39690D	<i>BnaAP2-4</i>	Cnn_random	1342	1362	431	6.41	47685.41	Nucleus	2
		BnaCnng71740D	<i>BnaAP2-5</i>	Cnn_random	578	598	227	7.87	25015.64	Nucleus	1
AT3G54990	<i>AthSMZ</i>	BnaA09g54740D	<i>BnaSMZ-1</i>	A09_random	953	973	343	9.42	38181.8	Cytoplasm	1
		BnaC06g15540D	<i>BnaSMZ-2</i>	C06	911	931	328	9.15	36790.23	Cytoplasm	1
		BnaC08g25840D	<i>BnaSMZ-3</i>	C08	956	976	344	9.39	38334.04	Cytoplasm	1
AT2G39250	<i>AthSNZ</i>	BnaC02g15640D	<i>BnaSNZ</i>	C02	–	–	128	6.27	14495.41	Cytoplasm	1
AT2G28550	<i>AthTOE1</i>	BnaA03g22100D	<i>BnaTOE1-1</i>	A03	1460	1480	436	6.51	47782.51	Cytoplasm. Nucleus	2
		BnaA07g13990D	<i>BnaTOE1-2</i>	A07	1512	1532	454	6.48	49570.20	Nucleus	2
		BnaC03g26480D	<i>BnaTOE1-3</i>	C03	1384	1404	417	6.61	45569.96	Cytoplasm. Nucleus	1
		BnaC04g15640D	<i>BnaTOE1-4</i>	C04	1496	1516	454	6.48	49308.84	Nucleus	2
		BnaC09g13430D	<i>BnaTOE1-5</i>	C09	694	714	103	8.09	11002.98	Nucleus	1
AT5G60120	<i>AthTOE2</i>	BnaA02g06490D	<i>BnaTOE2-1</i>	A02	1184	1204	431	8.56	47492.05	Cytoplasm. Nucleus	1
		BnaA10g12950D	<i>BnaTOE2-2</i>	A10	1412	1432	452	7.74	49305.81	Cytoplasm. Nucleus	1
		BnaC09g35430D	<i>BnaTOE2-3</i>	C09	1187	1207	454	7.74	49632.26	Cytoplasm. Nucleus	1
AT5G67180	<i>AthTOE3</i>	BnaA07g12050D	<i>BnaTOE3-1</i>	A07	1315	1335	360	8.91	40692.38	Nucleus	2
		BnaC07g16190D	<i>BnaTOE3-2</i>	C07	1272	1292	361	9.11	40835.46	Cytoplasm. Nucleus	2

49.63 kDa, and the PI values varied from 6.02 to 9.42. The predicted subcellular localization results showed that nine *euAP2* proteins were located in the nuclear region, four proteins were located in the cytoplasm region and the other six proteins were located in the nuclear and cytoplasm regions. These results indicate that different *euAP2* family proteins may perform different functions.

Four putative miR172 family members (*Bna-miR172a*, *Bna-miR172b*, *Bna-miR172c*, and *Bna-miR172d*) in *B. napus* were predicted in miRbase, their precursor and mature sequences were shown in Additional file 1: Table S1. Multiple sequence alignments of the miR172 precursor and mature sequences were shown in Additional file 8: Figure S1a, b. The four mature miR172 sequences were highly conserved except for the first base, whereas divergence was observed in the precursor sequences. The secondary structure of the *Bna-MIR172* gene transcript was

predicted by Mfold (Additional file 8: Figure S1c), and the four precursor sequences formed different stem-loop structures, which may lead to functional differences among members.

Target prediction for miRNAs is based on the high degree of homology between miRNAs and their target genes in plants [34]. Two target prediction servers, namely, TAPIR and psRNATarget, were used to identify potential targets of miR172 in *B. napus*. A total of 17 targets carrying the miRNA response element (MRE) for miR172 were predicted, and the position of miRNA binding sites were displayed in Table 1. A comparison of the *Bna-miR172* mature sequences to the *euAP2* sequences showed that 17 *euAP2s* contained sequences complementary to the *Bna-miR172* mature sequences, with one to three base mismatches (Fig. 1a). All the identified target sites of *Bna-miR172* were located in the coding regions of *euAP2* genes.



The chromosome distribution of the euAP2 genes and Bna-miR172 precursors is shown in Fig. 1b. The 19 euAP2s and four Bna-miR172s were located in 13 known chromosomes, and four were located in the scaffolds. These genes and miRNA precursors were unevenly distributed in the *B. napus* sub-genomes, with six and nine euAP2 genes located in the A and C genomes, respectively. The other four euAP2 genes mapped onto A01-random, A09-random, Ann-random and Cnn-random. The Bna-miR172 genes were distributed in A03, A09, C02, C03 and Ann_random. However, no euAP2 genes and Bna-miR172 precursors were located on A01, A04, A05, A06, A08, and C01 chromosomes. The absence of genes on the chromosomes and uneven distribution on the sub-genomes of euAP2 genes clarified their translocation during evolution.

Phylogenetic and selection pressure analysis of the euAP2 and Bna-miR172 genes

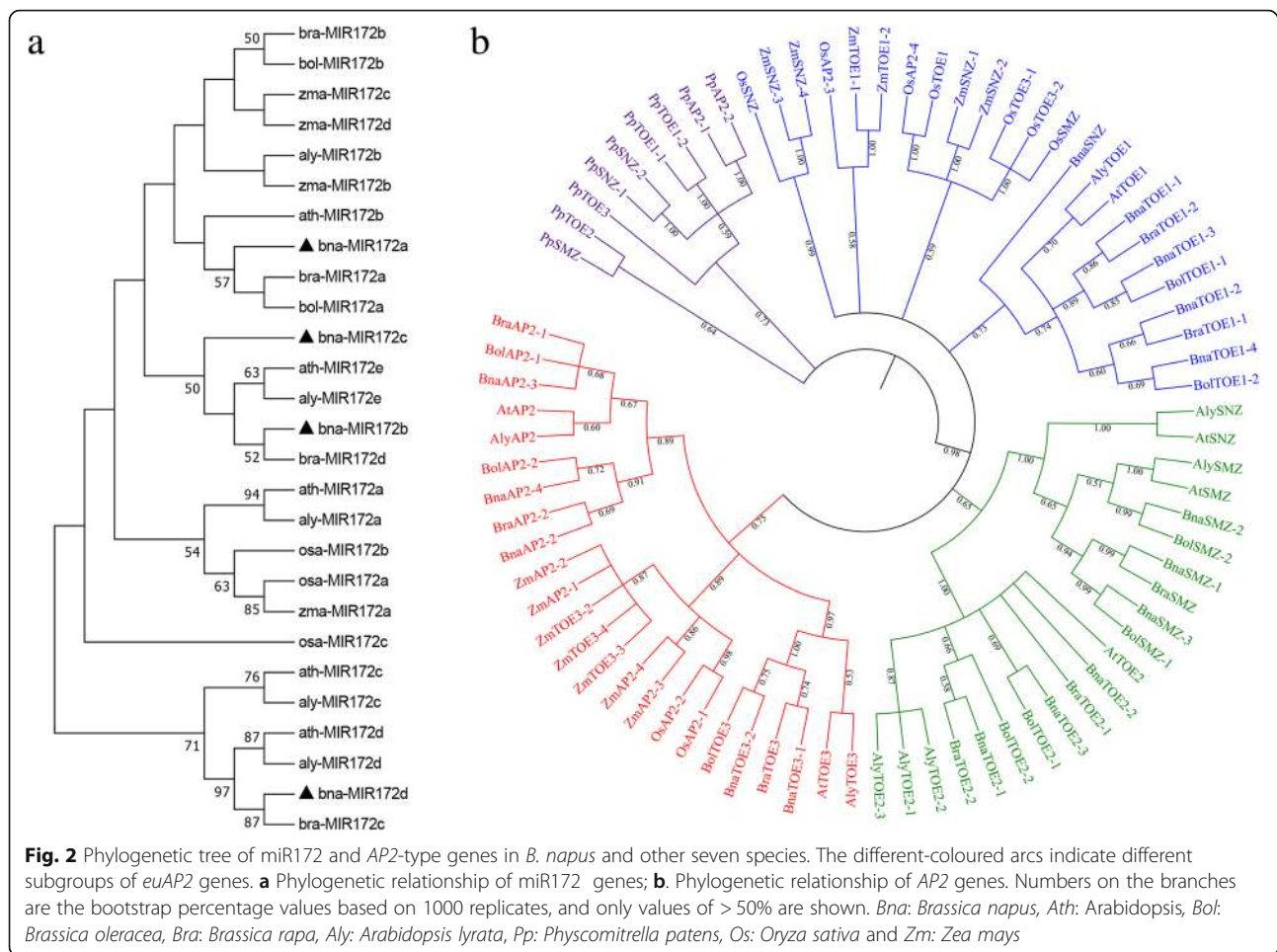
To evaluate the evolutionary relationships of the AP2 and miR172 gene members, an unrooted neighbour-joining phylogenetic tree was created using the precursor sequence of miR172 and amino acid sequences of AP2 genes from Arabidopsis, *B. napus*, *B. rapa*, *B. oleracea*, rice, maize, moss and *Arabidopsis lyrata*. However, no miR172 gene was identified in moss. MIR172 genes from other seven plant species could be classified into four groups according to the phylogenetic analysis. Every group had at least one MIR172 gene from Arabidopsis (Fig. 2a). The AP2 genes from the eight species were assigned to four groups according to the phylogenetic topology (Fig. 2b). The BnaAP2 genes were firstly clustered with AP2s from two progenitors of *B. napus*, followed by Arabidopsis and *A. lyrata*, which formed a specific Brassicaceae clade. EuAP2 proteins from rice exhibited closer relationships to maize and formed a

monocot clade. EuAP2 in dicot and monocot plants formed a larger clade together. The moss clustered into one independent clade. These results suggested that euAP2 protein may be highly conserved in monocot and dicot and diverged after the split between bryophytes and vascular plants.

We also predicted the paralogous and orthologous relationships of the AP2 proteins among Arabidopsis, *B. napus*, *B. rapa* and *B. oleracea*. Seven pairs of paralogs were identified in *B. napus*, and 11 pairs of putative orthologous proteins were identified between species. To explore the driving force of gene divergence after gene duplication, the nonsynonymous/synonymous substitution ratio (Ka/Ks) of euAP2 gene pairs was calculated (Table 2). With the exception of one gene pair (*BnaTOE1-1/BraTOE1-2*) with a Ka/Ks > 1, the majority of euAP2 gene pairs had a Ka/Ks < 1, suggesting that the AP2 gene family experienced strong purifying selective pressure during evolution.

We examined five types of gene duplications, namely, singleton, dispersed, proximal, tandem, and WGD or segmental duplication using the MCSanX program. No tandem repeat events within the euAP2 gene family were found, while five dispersed and 11 segmental duplication events were identified (Table 3). These results indicated that some euAP2 genes were probably generated by gene duplication and that the WGD or segmental duplication events were a major driving force of euAP2 evolution [35].

To further infer the phylogenetic relationships of the BnaAP2 family, we constructed three comparative syntentic maps of *B. napus* associated with Arabidopsis, *B. rapa* and *B. oleracea* (Fig. 3). A total of 13 BnaAP2 genes showed a syntenic relationship with those in Arabidopsis, followed by *B. rapa* (13) and *B. oleracea* (13). Interestingly, collinear (13 BnaAP2 genes) were identified between *B. napus* and the three other species, indicating



that these orthologous pairs may have already existed before divergence (Additional file 2: Table S2).

Structural organization and conserved domain analysis of *euAP2* genes

To gain further insights into the structure of the *euAP2* genes, we aligned their coding sequences to their genomic sequences (Additional file 9: Figure S2). The *euAP2* genes were classified into five subgroups. The difference in the number of exons (4 to 10), the intron length and the presence of an untranslated region (UTR) were assessed among the 19 genes, indicating that the AP2-type genes may perform different functions despite being in the same subfamily. However, the genes located at the end of the same branch always exhibited similar structures. The exon-intron structures were consistent with the phylogenetic relationships and conserved in each group, although some paralogous genes demonstrated some differences.

MEME was used to identify putative conserved motifs among the *euAP2* genes (Fig. 4). The 10 most conserved motifs were recognized, and the length of the motifs ranged from 11 to 50 amino acids. The motif annotations are listed

in Additional file 3: Table S3. Motifs 1 and 4 were annotated as the AP2-ERF domain, the other motifs had unknown functions. The conserved AP2 domain was created by WebLogo, and all the *euAP2* proteins contain one or both of motifs 1 and 4, which further confirmed the identification results presented in Table 1. Most of the *euAP2*s within the same groups contained a similar motif composition. The similar motif number and arrangements among the AP2-type proteins in the same subgroups indicated that the protein function was conserved within a specific subfamily. However, there were also some exceptions: *BnaAP2*–1 and *BnaAP2*–5 had 4 motifs (motifs 2, 4, 5, and 6); *BnaAP2*–3 had 7 motifs; *BnaAP2*–2 / *BnaAP2*–4 contained 8 motifs; *BnaSNZ* had only one AP2-ERF motif; and *BnaTOE1*–5 had only 2 motifs, which was far fewer than the number observed in other proteins of the same subfamily (9 motifs). Motifs 6 and 7 were unique in Clades I and V, respectively, and may be important for the functions of *BnaAP2* and *BnaTOE* proteins. These specific motifs and motif compositions may contribute to the functional divergence of *euAP2* genes.

In general, the similar gene structures and conserved motif compositions of *euAP2* members in the

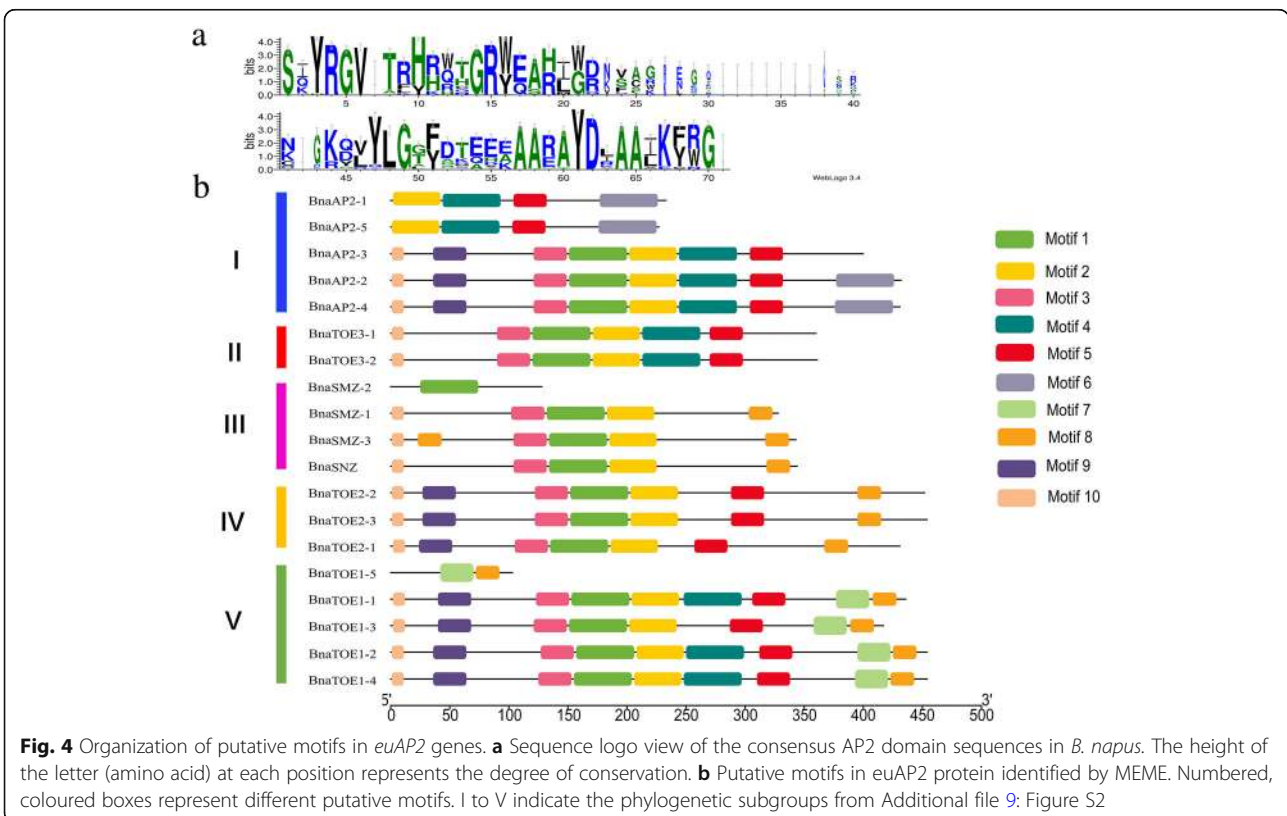
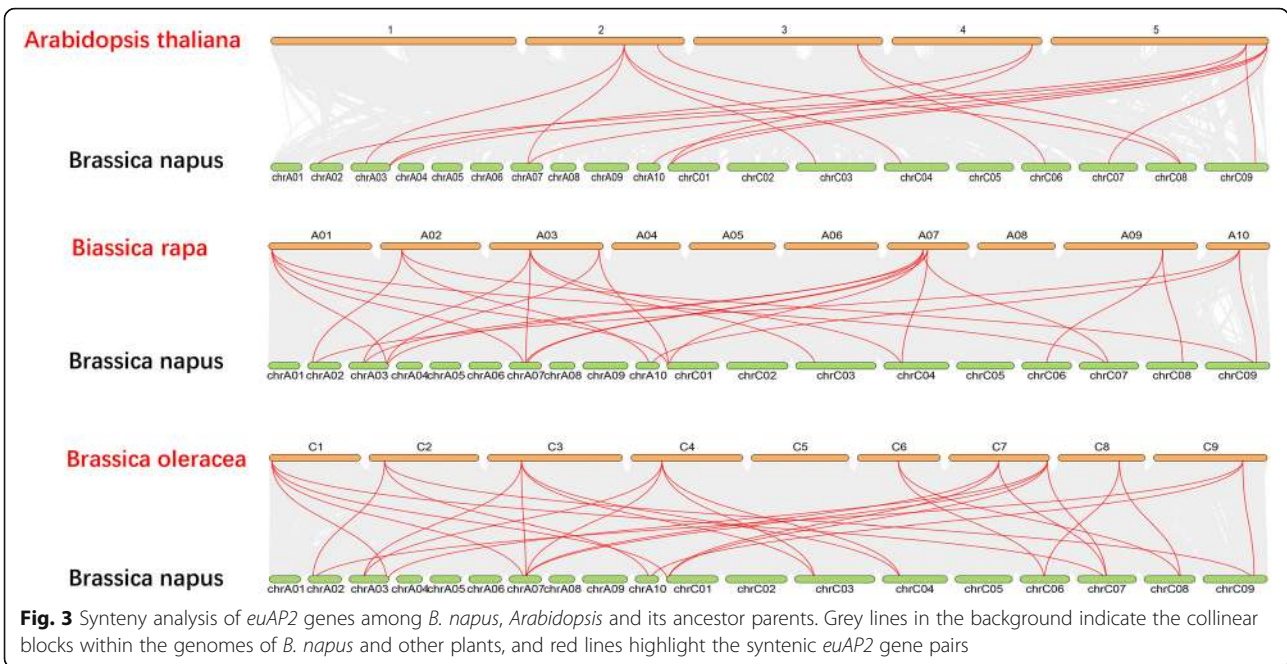
Table 2 Ka and Ks values for orthologous and paralogous gene pairs between *B.napus* and another three plant species

	Gene Name	Gene Name	Ka	Ks	Ka/Ks	Selection pressure
Orthologous	<i>BnaAP2-2</i>	<i>BraAP2-2</i>	0.001	0	NA	NA
	<i>BnaAP2-4</i>	<i>BolAP2-2</i>	0	0	NA	NA
	<i>BnaSMZ-1</i>	<i>BraSMZ</i>	0	0	NA	NA
	<i>BnaSMZ-2</i>	<i>BolSMZ-2</i>	0.0139	0.0209	0.6651	Purifying selection
	<i>BnaSMZ-3</i>	<i>BolSMZ-1</i>	0	0	NA	NA
	<i>BnaTOE1-1</i>	<i>BraTOE1-2</i>	0.4165	0.3333	1.2496	Positive selection
	<i>BnaTOE1-3</i>	<i>BolTOE1-1</i>	0.0116	0.0243	0.4774	Purifying selection
	<i>BnaTOE2-2</i>	<i>BraTOE2-1</i>	0.0077	0.0424	0.1816	Purifying selection
	<i>BnaTOE2-3</i>	<i>BolTOE2-1</i>	0.001	0	NA	NA
	<i>BnaTOE3-1</i>	<i>BraTOE3</i>	0.0012	0	NA	NA
	<i>BnaTOE3-2</i>	<i>BolTOE3</i>	0	0	NA	NA
	Paralogous	<i>BnaAP2-1</i>	<i>BnaAP2-5</i>	0.0076	0.0430	0.1767
<i>BnaAP2-2</i>		<i>BnaAP2-4</i>	0.0101	0.0485	0.2082	Purifying selection
<i>BnaSMZ-1</i>		<i>BnaSMZ-3</i>	0.0128	0.0256	0.5000	Purifying selection
<i>BnaTOE1-1</i>		<i>BnaTOE1-3</i>	0.0234	0.0716	0.3268	Purifying selection
<i>BnaTOE1-2</i>		<i>BnaTOE1-4</i>	0.0078	0.0853	0.0914	Purifying selection
<i>BnaTOE2-2</i>		<i>BnaTOE2-3</i>	0.0304	0.0943	0.3224	Purifying selection
<i>BnaTOE3-1</i>		<i>BnaTOE3-2</i>	0.048	0.1088	0.4412	Purifying selection

Table 3 Duplication type of *euAP2* gene pairs

Gene ID	Gene Name	Gene ID	Gene Name	Duplication Type
BnaA01g34730D	<i>BnaAP2-1</i>			Dispersed
BnaA03g53830D	<i>BnaAP2-2</i>	BnaC01g01710D	<i>BnaAP2-3</i>	WGD or Segmental
BnaCnng39690D	<i>BnaAP2-4</i>			Dispersed
BnaCnng71740D	<i>BnaAP2-5</i>			Dispersed
BnaA09g54740D	<i>BnaSMZ-1</i>	BnaC08g25840D	<i>BnaSMZ-3</i>	WGD or Segmental
BnaC06g15540D	<i>BnaSMZ-2</i>	BnaC08g25840D	<i>BnaSMZ-3</i>	WGD or Segmental
BnaC02g15640D	<i>BnaSNZ</i>			Dispersed
BnaA03g22100D	<i>BnaTOE1-1</i>	BnaA07g13990D	<i>BnaTOE1-2</i>	WGD or Segmental
BnaA03g22100D	<i>BnaTOE1-1</i>	BnaC03g26480D	<i>BnaTOE1-3</i>	WGD or Segmental
BnaA03g22100D	<i>BnaTOE1-1</i>	BnaC04g15640D	<i>BnaTOE1-4</i>	WGD or Segmental
BnaA07g13990D	<i>BnaTOE1-2</i>	BnaC04g15640D	<i>BnaTOE1-4</i>	WGD or Segmental
BnaC09g13430D	<i>BnaTOE1-5</i>			Dispersed
BnaA02g06490D	<i>BnaTOE2-1</i>	BnaA10g12950D	<i>BnaTOE2-2</i>	WGD or Segmental
BnaA02g06490D	<i>BnaTOE2-1</i>	BnaC09g35430D	<i>BnaTOE2-3</i>	WGD or Segmental
BnaA10g12950D	<i>BnaTOE2-2</i>	BnaC09g35430D	<i>BnaTOE2-3</i>	WGD or Segmental
BnaA07g12050D	<i>BnaTOE3-1</i>	BnaC07g16190D	<i>BnaTOE3-2</i>	WGD or Segmental

Dispersed means that the gene might arise from transposition, such as 'replicative transposition', 'non-replicative transposition' or 'conservative transposition'; WGD or segmental means that the gene might arise from Whole Genome Duplication or segmental duplication



same group as well as the results of the phylogenetic analysis, further confirm the reliability of the evolutionary classification.

Analysis of cis-regulatory elements (CREs) of *Bna-miR172* and *BnaAP2* genes

Temporal and spatial gene expression is regulated by the presence of different cis-regulatory elements in the promoters [36]. To understand the expression divergence, a 1000 bp region upstream of the transcription start site (TSS) of *euAP2* genes and a 1500 bp upstream of the *Bna-miR172* precursor sequences were extracted to analyse CREs using the PlantCARE database (Additional file 4: Table S4). The identified CREs were classified into five main categories based on their function: light-responsive elements, hormone-responsive elements, stress-responsive elements, growth and development-responsive elements, and others. All the promoter sequences contained a TATA-box and CAAT-box. Light-responsive elements such as G-Box, GAG-motif, Box 4, AAAC-motif and Box 1 were abundant in most genes. CRE such as ERE, ABRE TGA element, GARE-motif, P-box, and CGTCA and TGACG motifs were responsive to various plant hormones including ethylene, abscisic acid, auxin, gibberellin

and MeJA. Stress-responsive elements such as ARE, MBS, TC-rich repeats, LTR, Box-W1 and HSE have been reported in response to various abiotic stresses. In addition, other growth and development-responsive elements, such as the CCAAT-box, 5' UTR Py-rich stretch and CCGT CC-box were found to be associated with endosperm and meristem expression and circadian control. In general, the expression of *Bna-miR172* and its target *euAP2* genes could be regulated by diverse environments and internal developmental factors.

Different expression profiles of *euAP2* genes

Gene expression patterns in different tissues

To investigate the putative roles of *euAP2* genes, the expression patterns of all *euAP2s* were analysed in diverse tissues based on RNA-seq data (Fig. 5a). The *euAP2s* were classified into seven groups by using hierarchical clustering. The five *AP2* genes in the first group, i.e., *BnaTOE2-2*, *BnaTOE1-1*, *BnaTOE1-3*, *BnaTOE1-4* and *BnaTOE2-3*, were expressed at high levels in the young leaves from the seedling stage. The second group had three genes (*BnaTOE1-2*, *BnaSMZ-1*, and *BnaSMZ-3*) that were highly expressed in the young leaves from the seedling stage and 24 d after flowering. The

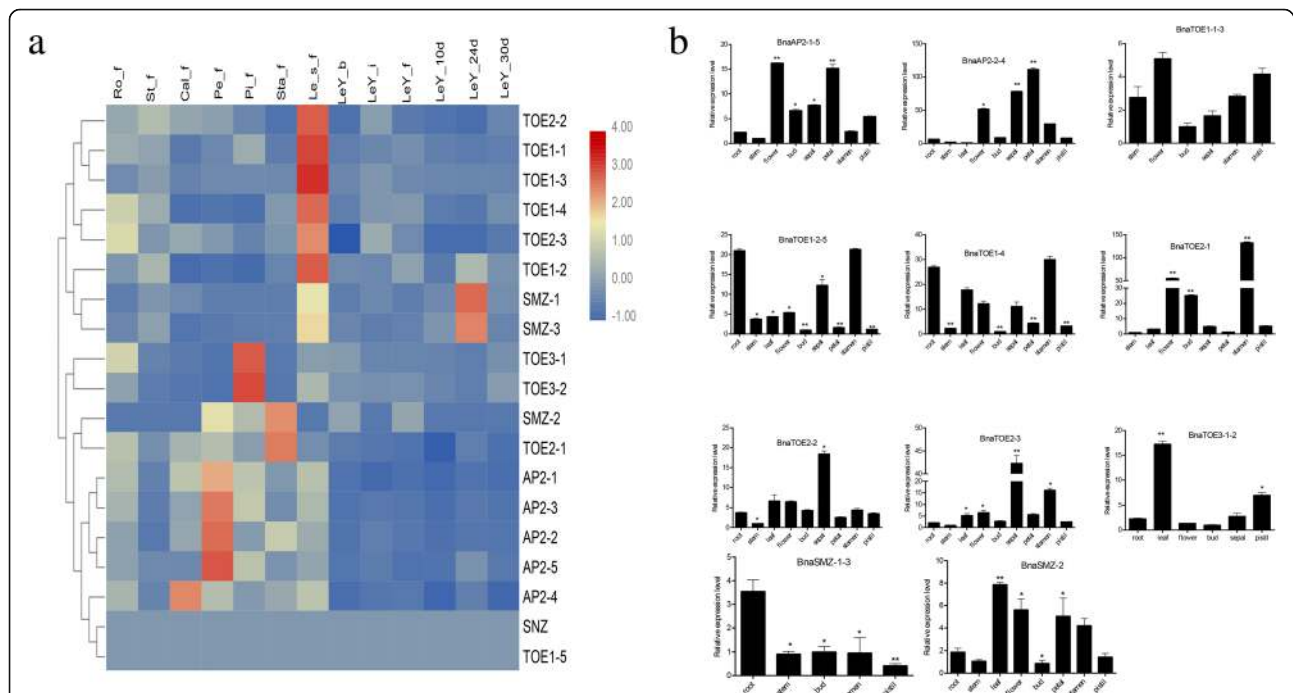


Fig. 5 Expression profiles of *euAP2* genes in different vegetative and reproductive tissues of ZS11. **a** Hierarchical clustering of expression profiles of the *euAP2* genes in 13 samples based on the ZS11 RNA-Seq data. Heatmap showing the log₂-transformed FPKM values. Tissues used for expression profiling are indicated at the top of each column. Every tissue has three replications. The genes are on the right of the expression bar. Ro-f, St-f, Cal-f, Pe-f, Pi-f and Sta-f represent root, stem, calyx, petal, pistil and stamen tissue collected from the full-bloom stage, respectively; Le_s-f, LeY-b, LeY-i, LeY-f, LeY-10d, LeY-24d and LeY-30d represent young leaves from the seedling stage, bud stage, early flowering stage, full-flowering stage, and 10 d, 24 d, and 30 d after flowering, respectively. **b** qRT-qPCR analysis of *euAP2* genes in nine tissues. Root as a control. Data were normalized to the *actin* gene, and error bars indicate the standard error (SE) of the mean. Student's *t*-test: **P* < 0.05, ***P* < 0.01

transcription of *euAP2* genes in the third to sixth groups was enriched in the pistils, stamens, sepals and calyxes, which indicated their potentially specialized function in floral organ development. *BnaSNZ* and *BnaTOE1-5* in the seventh group showed almost no expression in these tissues.

qRT-PCR was used to confirm the expression levels of the miR172 target *euAP2* genes in nine tissues (root, stem, leaf, flower, bud, sepal, petal, stamen and pistil) of ZS11 (Fig. 5b). Most of the *euAP2*s exhibited a distinct tissue-specific expression pattern and achieved significant differences compared with root. *BnaTOE1-2-5* and *BnaTOE1-4* displayed the highest transcript abundance in the root and stamen; *BnaTOE3-1-2* and *BnaSMZ-1-3* exhibited the highest expression in the leaf and root, respectively; *BnaTOE2-2* and *BnaTOE2-3* were specifically highly expressed in the sepal; and the other five *euAP2* genes (*BnaAP2-1-5*, *BnaAP2-2-4*, *BnaTOE1-1-3*, *BnaTOE2-1*, and *BnaSMZ-2*) exhibited increased expression in the floral organs (flower, bud, sepal, petal, stamen, and pistil), which indicating that these genes may be involved in the regulation of flowering time and floral organ development.

Gene expression patterns in early- and late-flowering lines

To investigate the putative *AP2* genes involved in flowering time regulation, the RNA-seq data from both early-flowering bulk material and late-flowering bulk material was extracted. First, the expression levels in the shoot tissues (S) and leaves (L) of early-flowering and late-flowering bulk materials at the vegetative stage were analysed (Additional file 10: Figure S3a). The *euAP2* expression patterns were divided into 3 categories between two tissues of the two lines. The first group showed no or low expression in the four samples and included *BnaSMZ-1*, *BnaSMZ-2*, *BnaSMZ-3*, *BnaTOE1-5* and *BnaTOE2-1*; the second group exhibited medium level expression and no obvious difference among the four samples and included *BnaTOE1-1*, *BnaTOE1-4*, *BnaTOE2-2*, *BnaTOE2-3*, *BnaAP2-2* and *BnaAP2-3*; and the third group exhibited relatively high expression in the four samples, *BnaAP2-1*, *BnaAP2-5*, *BnaTOE1-2* and *BnaTOE1-3* displayed higher expression in the late-flowering material than that in the early-flowering material in both shoot tissues (S) and leaves (L), which indicated their negative roles in flowering regulation, while *BnaAP2-4*, *BnaTOE3-1* and *BnaTOE3-2* did not show the above rules. Second, we further studied the RNA-seq data from juvenile leaves of the early-flowering material (18Z134) and late-flowering material (18Z88) at the vegetative and reproductive stages and obtained similar results (Additional file 10: Figure S3b). *BnaSMZ-1*, *BnaSMZ-2*, *BnaSMZ-3*, *BnaSNZ*, *BnaTOE1-1*, *BnaTOE1-5* and *BnaTOE2-1* belonged to the first group

and showed no or lower expression; *BnaTOE1-3*, *BnaTOE2-2*, *BnaTOE2-3*, *BnaTOE3-1* and *BnaTOE3-2* belonged to the second group and maintained a high expression level but exhibited no obvious difference among the four samples; *BnaAP2* (*AP2-1*, *AP2-2*, *AP2-3*, *AP2-4*, and *AP2-5*), *BnaTOE1-2* and *BnaTOE1-4* belonged to the third group and exhibited elevated expression in the vegetative-stage leaves and a higher transcript abundance in the late-flowering material than in the early-flowering material, which further confirmed their negative regulatory roles.

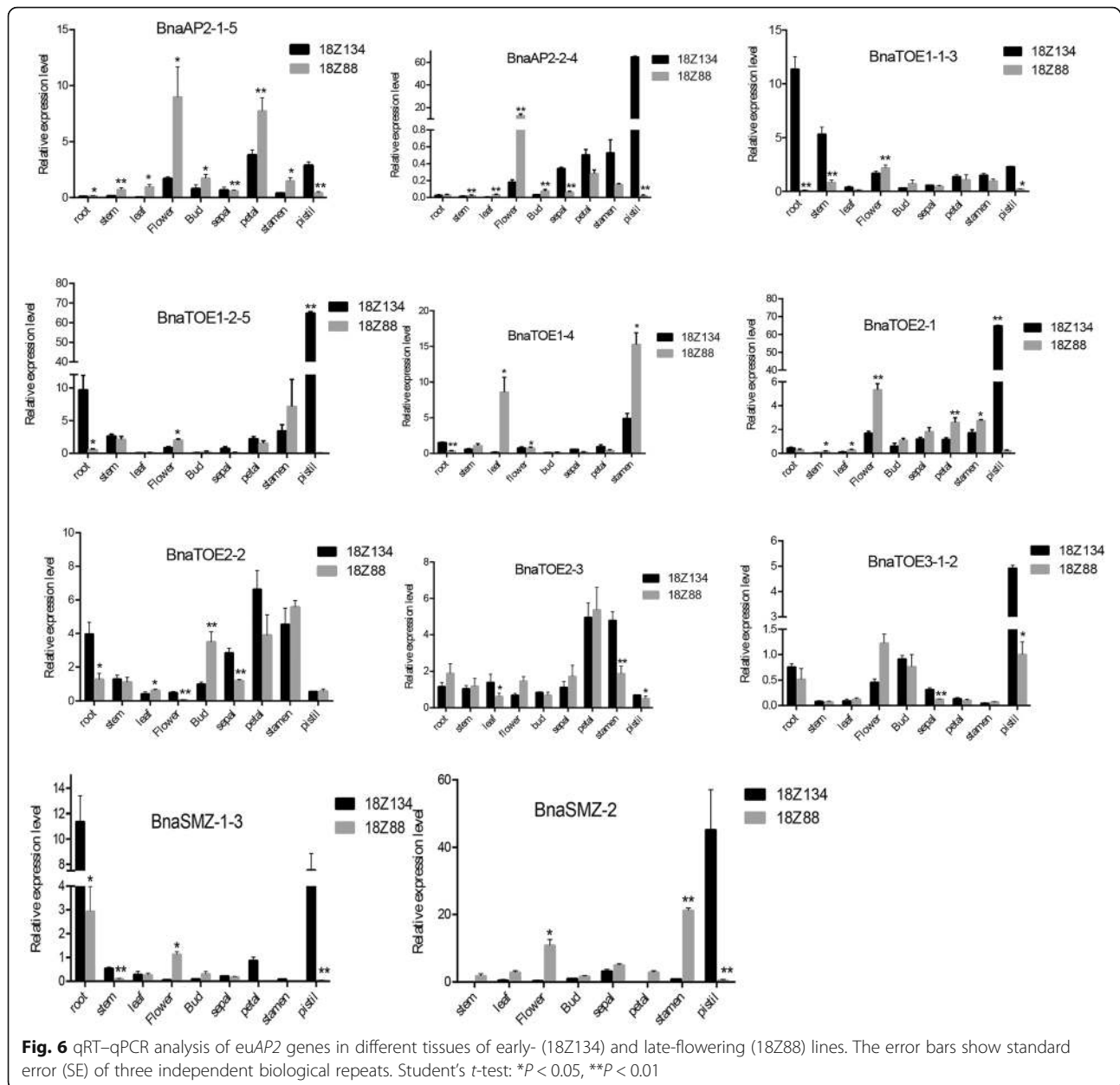
qRT-PCR was conducted to confirm the expression level of *AP2*s in the same materials (18Z88 and 18Z134) used for RNA-seq (Fig. 6). Most *euAP2* genes had higher expression levels in the floral organs of 18Z88 than 18Z134 and showed significant differences between them. A tissue-specific expression analysis revealed that *BnaTOE1-1-3*, *BnaTOE1-2-5*, *BnaTOE2-2* and *BnaSMZ-1-3* expressed abundantly in roots of 18Z134. All *euAP2* genes except *BnaTOE1-4* and *BnaTOE2-3* had higher expression levels in the pistil of 18Z134 than in 18Z88. The expression of *AP2*s in the other tissues presented relatively low expression in both lines.

Discussion

MiR172 and its target *AP2* genes in Brassica and their evolution

Transcription factors (TFs) play important roles in plant growth and development. The APETALA2/Ethylene Responsive Factor (*AP2/ERF*) proteins are a large family of TFs with a key function in response to biotic and abiotic stresses as well as developmental stages that have been identified in various plant species, including Arabidopsis [37], rice [38], *B. rapa* [39], *B. napus* [40, 41], barley and wheat [42], poplar [43] and soybean [44]. In this manuscript, we mainly focused on the *AP2* genes that belong to the *euAP2* group. The *euAP2* group in Arabidopsis includes six *AP2* genes (*AP2*, *TOE1*, *TOE2*, *TOE3*, *SMZ*, and *SNZ*). Each Arabidopsis *euAP2* gene has one to five orthologous genes in *B. napus*. In the present study, 19 *euAP2* genes were identified in *B. napus*, which is approximately more than twice the number identified in its progenitors *B. rapa* (8) and *B. oleracea* (9), indicating that some *euAP2* genes in *B. napus*, *B. rapa* and *B. oleracea* were subjected to a copy number increase due to WGD and polyploidization.

Based on the phylogenetic analysis, the *euAP2*s in *B. napus* can be classified into five groups (Additional file 9: Figure S2). Most *euAP2* genes in the same subgroup had similar exon-intron structures, although the exon number and intron length varied significantly among members of different subfamilies (Additional file 9: Figure S2). The majority of *euAP2* proteins belonging to the same group contained similar motif distributions, while *euAP2* proteins



had distinct motif constitutions and organizations among subgroups (Fig. 4b), a finding that was also reported by Song [40]. The divergence in gene structure and motif composition between *euAP2* genes suggests functional differentiation during evolution. The motif recognition and gene structure analysis also highly corroborated our phylogenetic classification. Most miRNA target genes identified in plants are TFs [45]. MiR172 is known to regulate the *euAP2* group of AP2-like TFs through transcript cleavage and translational repression in *Arabidopsis* [3, 21, 22]. In this study, 4 members of the miR172 family in *B. napus* were identified, and target prediction showed that 17 of the 19 *euAP2* genes contained a MRE for miR172 (Fig. 1a;

Table 1). Additionally, the miR172 binding site in the 3' coding region were also identified in the *AP2* genes of barley and some representative *euAP2* proteins [38, 42], suggesting that miR172 complementary sites in *euAP2* genes are conserved across plant species.

Duplicated type and synteny analyses of AP2 genes in *B. napus* and other species

Seven pairs of paralogs in *B. napus* and 11 pairs of orthologous proteins between species were identified via the phylogenetic analysis (Fig. 2b). Positive selection is the main driving force for functional divergence in *euAP2* proteins after gene duplication. A comparison of

the number of *euAP2* genes in *B. napus* with that in Arabidopsis and the ancestor parental genomes showed that *B. napus* has more genes (Fig. 3). Gene replication events that occurred during evolution contributed to the expansion of gene families [35]. Based on the duplication analysis, WGD or segmental duplication events had a major impact during *euAP2* evolution. Therefore, WGD or segmental duplication might be a possible reason for the increased number of *euAP2* genes.

Analysis of the expression patterns of *euAP2*s in *B. napus*

The spatio-temporal expression patterns of *euAP2*s have been analysed in many species. Jofuku showed that, unlike other floral homeotic genes, *AP2* is expressed in both nonfloral (stems and leaves) and floral tissues (sepals, petals, stamens, carpels, developing ovules and inflorescence meristems) in Arabidopsis [46]. Javier studied the expression of *AP2*-like genes in the roots, stems, young leaves, and spikes at various developmental stages in wheat and barley and showed that *AP2*-like genes were expressed in all tissues, peaked in the early stages of spike development and gradually decreased with spike maturation [42]. The *euAP2* genes in rice were transcribed in the juvenile and mature leaves, root tip, inflorescences and serial stages of the panicles [38]. The expression of *AP2/ERFs* in *B. napus* was also previously examined: Zhuang and Zhu surveyed *B. napus* EST databases and showed that *AP2/ERF* genes were highly expressed in the stems followed by flowers and leaves [47]; Hajar revealed that most of the *BnaAP2* subfamily showed high expression in the flower buds, roots, leaves, and stems via transcriptome sequencing [41]; Song used the RNA-seq data reported by Chahoub [32] and concluded that the *AP2* genes had higher gene expression in the roots than leaves [40].

Reports have indicated that the *AP2* genes have critical functions in flower ontogeny, including floral meristem establishment [27, 48–50], floral organ identity [3, 51, 52], and floral homeotic gene expression [44]. In this study, the *BnaAP2*s showed different expression patterns among tissues. More than half of the *euAP2* genes were expressed predominantly in reproductive organs such as the flowers, buds, sepals, petals, stamens, and pistils, suggesting that these *euAP2* genes also play important roles in floral development in *B. napus* [53].

To further validate whether the *euAP2* genes affect flowering time, we analysed their expression in different organs of early- and late-flowering lines. Certain *euAP2* genes, such as *BnaAP2-1*, *BnaAP2-5* and *BnaTOE1-2*, had higher expression levels in the floral organs of the late-flowering material (18Z88) than the early-flowering material (18Z134), indicating that they

may be floral suppressor genes. This observation was consistent with the findings of previous studies in Arabidopsis [21, 22, 27].

Conclusion

In this study, 19 *euAP2* genes and four miR172 members were identified in *B. napus* genome and the 19 *euAP2*s were categorized into five subgroups. The 17 *euAP2* genes, which were predicted to be targeted by miR172, have tissue specific expression patterns. Most of the *euAP2*s were highly expressed in the floral organs (sepals, petals, stamens, and pistils), suggesting that the *AP2*/miR172 module plays an important role in flower organ development. In addition, three genes, *BnaAP2-1*, *BnaAP2-5* and *BnaTOE1-2*, had higher expression levels in late-flowering lines than in early-flowering lines, which revealed that they might act as floral suppressors. Taken together, the identification and expression of miR172/*euAP2* genes provide insights for further research on the miR172/*euAP2* interaction and flower development in *B. napus*.

Materials and methods

Identification of *Bna*-miR172 and its target *euAP2* genes

The nucleotide and protein sequences of the *AP2* family genes from *A. thaliana*, *B. napus*, *B. rapa*, and *B. oleracea* were downloaded from the Arabidopsis Information Resource (TAIR, <http://www.arabidopsis.org>) and BRAD (<http://brassicadb.org/brad/index.php>). Sequences from *A. lyrata*, rice, maize and moss were obtained from EnsemblePlants (<http://plants.ensembl.org/index.html>). BLASTP searches were performed against the BRAD and EnsemblePlants database with default parameters using Arabidopsis *AP2* protein sequences as queries. Sequences with an E-value $\leq 10^{-10}$ were regarded as candidate proteins. To further confirm the candidate *euAP2* family genes, the presence of the *AP2* domain in the proteins was evaluated using the SMART (<http://smart.embl-heidelberg.de/>) [54] and Pfam (<http://pfam.xfam.org/>) [55] databases. To further validate the identified gene, the amino acid sequence of the identified genes were also submitted to the NCBI's conserved domain database (CDD, <https://www.ncbi.nlm.nih.gov/Structure/bwrpsb/bwrpsb.cgi>) and HMMER (<https://www.ebi.ac.uk/Tools/hmmer/search/hmmer>).

Physico-chemical parameters, including the theoretical isoelectric point (pI) and molecular weight (Mw) of the deduced proteins, were analysed using the ExPasy pI/Mw tool (<http://web.expasy.org/protparam/>) [56]. The subcellular localizations of the *AP2* family proteins were predicted using the Cell-PLoc website (<http://www.csbio.sjtu.edu.cn/bioinf/Cell-PLoc/>).

The precursor and mature sequences of the plant miRNA172 family were obtained from the miRbase22 database (<http://www.mirbase.org/>) [57]. The miR172 genes were named as assigned in miRbase (Bna-miR172) and with new serial numbers (such as a-e). The secondary structures of the Bna-miR172 precursors were predicted by the Mfold web server (<http://mfold.rna.albany.edu/?q=mfold>) [58]. The putative target genes of miR172 were searched via the web-based tools TAPIR (<http://bioinformatics.psb.ugent.be/webtools/tapir/>) [59] and psRNATarget (<http://plantgrn.noble.org/psRNATarget/>) [60] by simultaneously uploading the miR172 mature sequence and *euAP2* gene sequence with default parameters. Finally, the potential targets predicted by both servers with one or two AP2 conserved domains were selected as candidate target genes.

Chromosome positional information for the *euAP2* and miR172 genes was investigated by using the *B. napus* database (<http://www.genoscope.cns.fr/brassica-napus/>). The MapChart version 2.2 was used to map the *euAP2* and Bna-miR172 genes [61].

Phylogenetic and Ka/Ks analysis

Multiple sequence alignments of the protein sequences of the *euAP2* family genes and the precursor sequences of *miR172* were performed by ClustalW with default parameters [62]. The aligned sequences were then used to construct a neighbour-joining (NJ) tree by MEGA version 6.0 [63] with 1000 bootstrap replicates and pairwise deletion. The iTOL website (<https://itol.embl.de/>) was used to better visualize the phylogenetic tree [64]. The orthologous and paralogous relationships for *AP2* genes were inferred from the phylogenetic tree [65, 66]. The non-synonymous (Ka) and synonymous substitution rates (Ks) were calculated using DnaSp V6 software. Finally, the selection pressure experienced by gene pairs was assessed based on the Ka/Ks ratio [67].

Duplicated type and synteny analyses of *euAP2s* in *B. napus* and other species

The Multiple Collinearity Scan toolkit (MCScanX) was adopted to analyse the gene duplication events, with the default parameters [68]. To demonstrate the synteny relationship of *AP2* genes obtained from *B. napus* and the three other species, syntenic analysis maps were constructed using Dual Synteny Plotter software (<https://github.com/CJ-Chen/TBtools>) [69].

Analysis of exon–intron structure and motifs of *euAP2* genes

The exon–intron structures of the Brassica *euAP2* family genes were obtained by aligning coding sequences (CDSs) with their corresponding genomic sequences. The diagrams of exon–intron structure were created

using the online Gene Structure Display Server (GSDS 2.0: <http://gsds.cbi.pku.edu.cn>) [70].

The sequence logo of the euAP2 domains was plotted by WebLogo (<http://weblogo.berkeley.edu/logo.cgi>). A conserved motif analysis within the determined euAP2 family was performed by the MEME program (<http://meme-suite.org/>) with the following parameters: optimum width, 6–300 amino acids; number of repetitions of a motif, any; and maximum number of motifs, 10 [71]. The motif sequence annotations were analysed by InterPro (<https://www.ebi.ac.uk/interpro/beta/>) [72].

Analysis of cis-acting elements in the *B. napus* miR172 and *euAP2* gene promoters

The 1.5 kb upstream of the predicted transcription start site of Bna-miR172 precursor sequences and 1 kb upstream sequences of the euAP2 transcription start site were selected as the promoter regions. The intercepted promoter region was analysed for cis-regulatory elements using PlantCare (<http://bioinformatics.psb.ugent.be/webtools/plantcare/html/>) [73].

Plant materials

The RNA-seq data were generated from 13 different tissues of the sequenced *B. napus* var. Zhongshuang 11 (ZS11) from the Oil Crop Research Institute, CAAS (root, stem, calyx, petal, pistil and stamen collected during the full-bloom stage, young leaves from the seedling stage, bud stage, early flowering stage, full-flowering stage, and 10 d, 24 d, and 30 d after flowering) (BioProject ID, PRJNA358784). The extremely early- and late-flowering materials were selected from the recombinant inbred line (RIL) constructed by our laboratory [74]. The flowering time of them were listed in Additional file 5: Table S5. The expression data from shoot tissues (S) and leaves (L) of early-flowering bulk materials (18Z43, 18Z71 and 18Z134) and late-flowering bulk materials (18Z44, 18Z88 and 18Z163) at the vegetative stage were collected, and the accession number was SRP108958. In addition, RNA-seq data from the juvenile leaves of early-flowering material (18Z134) and late-flowering material (18Z88) at the vegetative and reproductive stages were also analysed and the accession number was PRJNA540020. Two independent biological replicates were analyzed per sample. The transcript abundance of the *euAP2* genes was calculated using fragments per kilobase of exon model per million mapped reads (FPKM). The log₂-transformed FPKM values were used to study *euAP2* gene expression (Additional file 6: Table S6).

Tissue-specific expression analysis

ZS11, 18Z134 and 18Z88 were used for the expression analysis. Five vegetative tissues (root, stem, leaf, flower, and bud) and four floral organs (sepal, petal, stamen and pistil) were collected at the same developmental stage for the qRT-PCR. All plant materials were planted in the experimental field of Southwest University, Chongqing, China.

Total RNA was extracted from all samples with an RNAeasy extraction kit (Invitrogen, Carlsbad, CA, USA) according to the manufacturer's instructions. The quality of RNA was assessed using an Agilent 2100 Bioanalyzer (Agilent, Böblingen, Germany) and examined through electrophoresis on a 1.5% agarose gel. For qRT-PCR, 1 µg of RNA was reverse transcribed into first-strand cDNA using a SuperScript™ First-Strand Synthesis System III (Invitrogen). Quantitative real-time PCR was performed with SYBR Green PCR Supermix on a real-time PCR machine (Bio-Rad, Hercules, CA, USA). The relative gene expression levels were calculated using the $2^{-\Delta\Delta C_t}$ method, with *BnaACTIN7* used as an internal control [75]. The qPCR primers are listed in Additional file 7: Table S7. At least two biological replicates were used, with three technical replicates performed for each sample.

Additional files

Additional file 1 : Table S1 The miR172 precursor and mature sequences identified in the *B.napus* genome. (XLSX 9 kb)

Additional file 2 : Table S2 Collinear *euAP2* gene pairs among *B. napus*, *Arabidopsis* and its ancestor parents (*B.rapa* and *B. oleracea*). (XLSX 12 kb)

Additional file 3 : Table S3 Annotation of putative motifs of *euAP2* proteins identified by MEME (XLSX 9 kb)

Additional file 4 : Table S4 Cis-regulatory elements predicted in the promoter region of *Bna-miR172* and *euAP2* genes (XLSX 11 kb)

Additional file 5 : Table S5 Flowering time of extreme material in 5 years of Chongqing (XLSX 9 kb)

Additional file 6 : Table S6 RNA-seq data of *euAP2* genes in various tissues of ZS11 and in leaf and shoot tissues of early- and late-flowering lines (XLSX 15 kb)

Additional file 7 : Table S7 Primers used for qRT-PCR of *euAP2* genes in *B.napus* (XLSX 10 kb)

Additional file 8 : Figure S1 Multiple sequence alignment of the *bna-miR172* mature sequence and precursor sequence and its secondary structures. **a** Multiple sequence alignment of the *bna-miR172* mature sequence; **b** Multiple sequence alignment of the *bna-miR172* precursor sequence; **c** Secondary structures of the pre-miR172 sequence in *B. napus*. (TIF 4456 kb)

Additional file 9 : Figure S2 Phylogenetic tree and gene structure of *euAP2* genes in *B. napus*. Subtree branch lines are coloured to indicate different clades. Blue boxes indicate untranslated 5' and 3' regions; yellow boxes indicate exons; black lines indicate introns. CDS, coding sequence; UTR, untranslated region. (TIF 1769 kb)

Additional file 10 : Figure S3 Expression profiles of *euAP2* genes in the early- and late-flowering lines based on RNA-Seq data. Hierarchical clustering results are shown on the left of the heat map and the

coloured scale bar on the right side of the map represents log₂-transformed FPKM values. Every sample has two replications. **a** Expression profiles of *euAP2* genes in leaf and shoot tissues. EL, leaves of early-flowering material; LL, leaves of late-flowering material; ES, shoot apical regions of early-flowering material; and LS, shoot apical regions of late-flowering material. **b** Expression profiles of *euAP2* genes in leaves at the vegetative and reproductive stages. EV, leaves of early-flowering material at the vegetative stage; LV, leaves of late-flowering material at the vegetative stage; ER, leaves of early-flowering material at the reproductive stage; and LR, leaves of late-flowering material at the reproductive stage. (TIF 2402 kb)

Abbreviations

AP2: *APETALA2*; *CRE*: Cis-regulatory elements; *FPKM*: Fragments per kilobase of exon per million fragments mapped; *Ka*: The ratio of the number of nonsynonymous substitutions per non-synonymous site; *Ka/Ks*: The nonsynonymous/synonymous substitution ratio; *Ks*: The ratio of the number of synonymous substitutions per synonymous site; *MRE*: MiRNA response element; *qRT-PCR*: quantitative real-time polymerase chain reaction; *SMZ*: *SCHLAFMUTZE*; *SNZ*: *SCHNARCHZAPPEN*; *TOE*: *TARGET OF EAT 1*; *WGD*: whole genome duplication

Acknowledgements

We are grateful to Kun Lu from Southwest University for kindly providing us the expression data.

Authors' contributions

WTY and LLZ conceived and designed the experiments; WTY conducted the data analysis and wrote the manuscript; LJN, XXF, and LK participated in drafting partial manuscript and revised the paper; JHJ and WJ performed phylogenetic analyses; PXX, CYR, GYM and TYC performed RNA extraction and qRT-PCR. All authors read and approved the final manuscript.

Funding

This work was supported by the National Natural Science Foundation of China (31771830, 31701335), National Key Research and Development Program of China (2016YFD0100202), the Fundamental Research Funds for Central Universities (XDJK2017A009), the Chongqing Science and Technology Commission (cstc2016shmszx80083) and the "111" Project (B12006). The funding body participated in the design of the study, provided experimental materials and funded the transcriptome analysis.

Availability of data and materials

All supporting data can be found within the manuscript and its additional supporting files.

Ethics approval and consent to participate

Not applicable.

Consent for publication

Not applicable.

Competing interests

The authors declare that they have no competing interests.

Received: 24 December 2018 Accepted: 11 July 2019

Published online: 01 August 2019

References

- Bartel D. MicroRNAs: genomics, biogenesis, mechanism, and function. *Cell*. 2007;116:281–97.
- Curaba J, Singh MB, Bhalla PL. miRNAs in the crosstalk between phytohormone signalling pathways. *J Exp Bot*. 2014;65(6):1425.
- Aukerman MJ, Sakai H. Regulation of flowering time and floral organ identity by a microRNA and its APETALA2-like target genes. *Plant Cell*. 2003;15(11):2730–41.
- Palatnik JF, Allen E, Wu X, Schommer C, Schwab R, Carrington JC, Weigel D. Control of leaf morphogenesis by microRNAs. *Nature*. 2003;425(6955):257.
- Fujii H, Chiou TJ, Lin SJ, Aung K, Zhu JK. A miRNA involved in phosphate-starvation response in *Arabidopsis*. *Curr Biol*. 2005;15(22):2038–43.

6. Zhao B, Ge L, Liang R, Li W, Ruan K, Lin H, Jin Y. Members of miR-169 family are induced by high salinity and transiently inhibit the NF-YA transcription factor. *BMC Mol Biol.* 2009;10(1):1–10.
7. Huijser P, Schmid M. The control of developmental phase transitions in plants. *Development.* 2011;138(19):4117–29.
8. Poethig RS. Small RNAs and developmental timing in plants. *Curr Opin Genet Dev.* 2009;19(4):374–8.
9. Fornara F, Coupland G. Plant phase transitions make a SPLash. *Cell.* 2009;138(4):625–7.
10. Chuck G, Hake S. Regulation of developmental transitions. *Curr Opin Plant Biol.* 2005;8(1):67–70.
11. Zhou CM, Wang JW. Regulation of flowering time by microRNAs. *J Genet Genomics.* 2013;40(5):211–5.
12. Spanudakis E, Jackson S. The role of microRNAs in the control of flowering time. *J Exp Bot.* 2014;65(2):365–80.
13. Srikanth A, Schmid M. Regulation of flowering time: all roads lead to Rome. *Cell Mol Life Sci.* 2011;68(12):2013–37.
14. Wang JW, Czech B, Weigel D. MIR156-regulated SPL transcription factors define an endogenous flowering pathway in *Arabidopsis thaliana*. *Cell.* 2009;138(4):738–49.
15. Wu G, Park MY, Conway SR, Wang JW, Weigel D, Poethig RS. The sequential action of miR156 and miR172 regulates developmental timing in *Arabidopsis*. *Cell.* 2009;138(4):750–9.
16. Yamaguchi A, Wu MF, Yang L, Wu G, Poethig RS, Wagner D. The microRNA-regulated SBP-box transcription factor SPL3 is a direct upstream activator of *LEAFY*, *FRUITFULL*, and *APETALA1*. *Dev Cell.* 2009;17(2):268–78.
17. Wu G, Poethig RS. Temporal regulation of shoot development in *Arabidopsis thaliana* by miR156 and its target *SPL3*. *Development.* 2006;133(18):3539–47.
18. Mathieu J, Yant LJ, Mürdtter F, Küttner F, Schmid M. Repression of flowering by the miR172 target *SMZ*. *PLoS Biol.* 2009;7(7):e1000148.
19. Zhu QH, Helliwell CA. Regulation of flowering time and floral patterning by miR172. *J Exp Bot.* 2011;62(2):487–95.
20. Park W, Li J, Song R, Messing J, Chen X. CARPEL FACTORY, a dicer homolog, and HEN1, a novel protein, act in microRNA metabolism in *Arabidopsis thaliana*. *Curr Biol.* 2002;12(17):1484–95.
21. Schmid M, Uhlenhaut NH, Godard F, Demar M, Bressan R, Weigel D, Lohmann JU. Dissection of floral induction pathways using global expression analysis. *Development.* 2003;130(24):6001–12.
22. Chen X. A microRNA as a translational repressor of *APETALA2* in *Arabidopsis* flower development. *Science.* 2004;303(5666):2022–5.
23. Okamoto JK, Caster B, Villarreal R, Montagu MV, Jofuku KD. The AP2 domain of *APETALA2* defines a large new family of DNA binding proteins in *Arabidopsis*. *Proc Natl Acad Sci U S A.* 1997;94(13):7076–81.
24. Jung JH, Seo YH, Seo PJ, Reyes JL, Ju Y, Chua NH, Park CM. The *GIGANTEA*-regulated microRNA172 mediates photoperiodic flowering independent of *CONSTANS* in *Arabidopsis*. *Plant Cell.* 2007;19(9):2736–48.
25. Martin A, Adam H, Díazmendoza M, Żurczak M, Gonzálezschain ND, Suárezlópez P. Graft-transmissible induction of potato tuberization by the miR172. *Development.* 2009;136(17):2873–81.
26. Jung JH, Seo PJ, Kang SK, Park CM. MiR172 signals are incorporated into the miR156 signaling pathway at the *SPL3/4/5* genes in *Arabidopsis* developmental transitions. *Plant Mol Biol.* 2011;76(1–2):35.
27. Yant L, Mathieu J, Dinh TT, Ott F, Lanz C, Wollmann H, Chen X, Schmid M. Orchestration of the floral transition and floral development in *Arabidopsis* by the bifunctional transcription factor *APETALA2*. *Plant Cell.* 2010;22(7):2156–70.
28. Lauter N, Kampani A, Carlson S, Goebel M, Moose SP, Freeling M. MicroRNA172 down-regulates *glossy15* to promote vegetative phase change in maize. *Proc Natl Acad Sci U S A.* 2005;102(26):9412–7.
29. Zhu QH, Upadhyaya NM, Gubler F, Helliwell CA. Over-expression of miR172 causes loss of spikelet determinacy and floral organ abnormalities in rice (*Oryza sativa*). *BMC Plant Biol.* 2009;9(1):149.
30. Mlotshwa S, Yang Z, Kim Y, Chen X. Floral patterning defects induced by *Arabidopsis APETALA2* and microRNA172 expression in *Nicotiana benthamiana*. *Plant Mol Biol.* 2006;61(4–5):781–93.
31. Nair SK, Wang N, Turuspekov Y, Pourkheirandish M, Sinsuwongwat S, Chen GX, Sameri M, Tagiri A, Honda I, Watanabe Y. Cleistogamous flowering in barley arises from the suppression of microRNA-guided HvAP2 mRNA cleavage. *Proc Natl Acad Sci U S A.* 2010;107(1):490–5.
32. Chalhoub B, Denoeud F, Liu S, Parkin IAP, Tang H, Wang X, Chiquet J, Belcram H, Tong C, Samans B. Early allopolyploid evolution in the post-Neolithic *Brassica napus* oilseed genome. *Science.* 2014;345(6199):950–3.
33. Nova-Franco B, Íñiguez LP, Valdés-López O, Alvarado-Affantranger X, Lejía A, Fuentes SI, Ramírez M, Paul S, Reyes JL, Girard L. The micro-RNA172c-*APETALA2*-1 node as a key regulator of the common bean-rhizobium etli nitrogen fixation symbiosis. *Plant Physiol.* 2015;168(1):273–91.
34. Fahlgren N, Carrington JC. MiRNA target prediction in plants. *Methods Mol Biol.* 2010;592:51–7.
35. Cannon SB, Mitra A, Baumgarten A, Young ND, May G. The roles of segmental and tandem gene duplication in the evolution of large gene families in *Arabidopsis thaliana*. *BMC Plant Biol.* 2004;4(1):10.
36. Hernandez-Garcia CM, Finer JJ. Identification and validation of promoters and cis-acting regulatory elements. *Plant Sci.* 2014;217–218(1):109–19.
37. Nakano T, Suzuki K, Fujimura T, Shinshi H. Genome-wide analysis of the *ERF* gene family in *Arabidopsis* and Rice. *Plant Physiol.* 2006;140(2):411.
38. Tang M, Li G, Chen M. The phylogeny and expression pattern of *APETALA2*-like genes in Rice. *J Genet Genomics.* 2007;34(10):930–8.
39. Song X, Li Y, Hou X. Genome-wide analysis of the AP2/ERF transcription factor superfamily in Chinese cabbage (*Brassica rapa* ssp. *pekinensis*). *BMC Genomics.* 2013;14(1):573.
40. Song X, Wang J, Ma X, Li Y, Lei T, Wang L, Ge W, Guo D, Wang Z, Li C. Origin, expansion, evolutionary trajectory, and expression bias of AP2/ERF superfamily in *Brassica napus*. *Front Plant Sci.* 2016;7(307):1186.
41. Owji H, Hajiebrahimi A, Seradj H, Hemmati S. Identification and functional prediction of stress responsive AP2/ERF transcription factors in *Brassica napus* by genome-wide analysis. *Comput Biol Chem.* 2017;71:32.
42. Gilhumanes J, Pistón F, Martín A, Barro F. Comparative genomic analysis and expression of the *APETALA2*-like genes from barley, wheat, and barley-wheat amphiploids. *BMC Plant Biol.* 2009;9(1):66.
43. Zhuang J, Cai B, Peng RH, Zhu B, Jin XF, Xue Y, Gao F, Fu XY, Tian YS, Zhao W. Genome-wide analysis of the AP2/ERF gene family in *Populus trichocarpa*. *Febs Open Bio.* 2015;5(1):132–7.
44. Zhang G, Chen M, Chen X, Xu Z, Guan S, Li LC, Li A, Guo J, Mao L, Ma Y. Phylogeny, gene structures, and expression patterns of the ERF gene family in soybean (*Glycine max* L.). *J Exp Bot.* 2008;59(15):4095–107.
45. Rhoades MW, Reinhart BJ, Lim LP, Burge CB, Bartel B, Bartel DP. Prediction of plant microRNA targets. *Cell.* 2002;110(4):513–20.
46. Jofuku KD, Boer BGD, Montagu MV, Okamoto JK. Control of *Arabidopsis* flower and seed development by the homeotic gene *APETALA2*. *Plant Cell.* 1994;6(9):1211–25.
47. Zhuang J, Zhu B. Analysis of *Brassica napus* ESTs: gene discovery and expression patterns of AP2/ERF-family transcription factors. *Mol Biol Rep.* 2014;41(1):45–56.
48. Irish VF, Sussex IM. Function of the *apetala-1* gene during *Arabidopsis* floral development. *Plant Cell.* 1990;2(8):741–53.
49. Bowman JL, Alvarez J, Weigel D, Meyerowitz EM, Smyth DR. Control of flower development in *Arabidopsis thaliana* by *APETALA1* and interacting genes. *Development.* 1993;119(3):721–43.
50. Schultz EA, Haughn GW. Genetic analysis of the floral initiation process (FLIP) in *Arabidopsis*. *Development.* 1993;119(3):745–65.
51. Kunst L, Klenz JE, Martínez-Zapater J, Haughn GW. AP2 gene determines the identity of perianth organs in flowers of *Arabidopsis thaliana*. *Plant Cell.* 1989;1(12):1195–208.
52. Bowman JL, Smyth DR, Meyerowitz EM. Genes directing flower development in *Arabidopsis*. *Plant Cell.* 1989;1(1):37–52.
53. Lohmann JU, Weigel D. Negative regulation of the *Arabidopsis* homeotic gene *AGAMOUS* by the *APETALA2* product. *Cell.* 1991;65(6):991–1002.
54. Letunic I, Doerks T, Bork P. SMART 7: recent updates to the protein domain annotation resource. *Nucleic Acids Res.* 2012;40(Database issue):302–5.
55. Finn RD, Bateman A, Clements J, Coggill P, Eberhardt RY, Eddy SR, Heeger A, Hetherington K, Holm L, Mistry J. Pfam: the protein families database. *Nucleic Acids Res.* 2014;42(Database issue):222–30.
56. Gasteiger E, Hoogland C, Gattiker A, Duvaud SE, Wilkins MR, Appel RD, Bairoch A. Protein identification and analysis tools on the ExPASy server: Humana press; 2005.
57. Kozomara A, Griffiths-Jones S. MiRBase: annotating high confidence microRNAs using deep sequencing data. *Nucleic Acids Res.* 2014;42(Database issue):D68.
58. Zuker M. Mfold web server for nucleic acid folding and hybridization prediction. *Nucleic Acids Res.* 2003;31(13):3406–15.
59. Bonnet E, He Y, Billiau K, Van YDP. TAPIR, a web server for the prediction of plant microRNA targets, including target mimics. *Bioinformatics.* 2010;26(12):1566–8.

60. Dai X, Zhao PX. PsRNATarget: a plant small RNA target analysis server. *Nucleic Acids Res.* 2011;39:W155.
61. Voorrips RE. MapChart: software for the graphical presentation of linkage maps and QTLs. *J Hered.* 2002;93(1):77–8.
62. Larkin MA, Blackshields G, Brown NP, Chenna R, Mcgettigan PA, Mcwilliam H, Valentin F, Wallace IM, Wilm A, Lopez R. Clustal W and Clustal X version 2.0. *Bioinformatics.* 2007;23(21):2947–8.
63. Tamura K, Peterson D, Peterson N, Stecher G, Nei M, Kumar S. MEGA5: molecular evolutionary genetics analysis using maximum likelihood, evolutionary distance, and maximum parsimony methods. *Mol Biol Evol.* 2011;28(10):2731.
64. Letunic I, Bork P. Interactive tree of life (iTOL) v3: an online tool for the display and annotation of phylogenetic and other trees. *Nucleic Acids Res.* 2016;44:W242–5.
65. Song A, Gao T, Li P, Chen S, Guan Z, Wu D, Xin J, Fan Q, Zhao K, Chen F. Transcriptome-wide identification and expression profiling of the DOF transcription factor gene family in *Chrysanthemum morifolium*. *Front Plant Sci.* 2016;7(164):199.
66. Yang Z, Wang X, Gu S, Hu Z, Xu H, Xu C. Comparative study of SBP-box gene family in Arabidopsis and rice. *Gene.* 2008;407(1):1–11.
67. Rozas J, Ferrer-Mata A, Sánchez-DelBarrio JC, Guirao-Rico S, Librado P, Ramos-Onsins SE, Sánchez-Gracia A. DnaSP 6: DNA sequence polymorphism analysis of large data sets. *Mol Biol Evol.* 2017;34(12):3299–302.
68. Wang Y, Tang H, DeBarry JD, Tan X, Li J, Wang X, Lee T-H, Jin H, Marler B, Guo H, et al. MCScanX: a toolkit for detection and evolutionary analysis of gene synteny and collinearity. *Nucleic Acids Res.* 2012;40(7):e49.
69. Tao X, Chen C, Li C, Liu J, Liu C, He Y. Genome-wide investigation of *WRKY* gene family in pineapple: evolution and expression profiles during development and stress. *BMC Genomics.* 2018;19(1):490.
70. Hu B, Jin J, Guo AY, Zhang H, Luo J, Gao G. GSDS 2.0: an upgraded gene feature visualization server. *Bioinformatics.* 2014;31(8):1296.
71. Bailey TL, Johnson J, Grant CE, Noble WS. The MEME suite. *Nucleic Acids Res.* 2015;43:W39–49.
72. Finn RD, Attwood TK, Babbitt PC, Bateman A, Bork P, Bridge AJ, Chang HY, Dosztányi Z, Elgebalí S, Fraser M. InterPro in 2017—beyond protein family and domain annotations. *Nucleic Acids Res.* 2017;45(Database issue):D190–9.
73. Lescot M, Déhais P, Thijs G, Marchal K, Moreau Y, Peer YVD, Rouz P, Rombauts S. PlantCARE, a database of plant cis-acting regulatory elements and a portal to tools for in silico analysis of promoter sequences. *Nucleic Acids Res.* 2002;30(1):325–7.
74. Liu L, Qu C, Wittkop B, Yi B, Xiao Y, He Y, Snowdon RJ, Li J. A high-density SNP map for accurate mapping of seed fibre QTL in *Brassica napus* L. *PLoS One.* 2013;8(12):e83052.
75. Livak KJ, Schmittgen TD. Analysis of relative gene expression data using real-time quantitative PCR and the $2^{-\Delta\Delta Ct}$ method. *Methods.* 2001;25(4):402–8.

Publisher's Note

Springer Nature remains neutral with regard to jurisdictional claims in published maps and institutional affiliations.

Ready to submit your research? Choose BMC and benefit from:

- fast, convenient online submission
- thorough peer review by experienced researchers in your field
- rapid publication on acceptance
- support for research data, including large and complex data types
- gold Open Access which fosters wider collaboration and increased citations
- maximum visibility for your research: over 100M website views per year

At BMC, research is always in progress.

Learn more biomedcentral.com/submissions

